

# *In vitro* anthelmintic activity of an R-carvone nanoemulsions towards multiresistant *Haemonchus contortus*

## Research Article

**Cite this article:** Aguiar AARM *et al* (2022). *In vitro* anthelmintic activity of an R-carvone nanoemulsions towards multiresistant *Haemonchus contortus*. *Parasitology* **149**, 1631–1641. <https://doi.org/10.1017/S0031182022001135>

Received: 11 May 2022

Revised: 29 July 2022

Accepted: 5 August 2022



First published online: 2 September 2022

### Key words:

Carvone; nanoemulsion; nematodes; phytotherapy; sodium alginate

### Author for correspondence:

Claudia Maria Leal Bevilaqua,  
E-mail: [bevilaqua.uece@gmail.com](mailto:bevilaqua.uece@gmail.com)

Antônia Aniellen Raienne Moises Aguiar<sup>1</sup>, José Vilemar de Araújo Filho<sup>1</sup>, Henety Nascimento Pinheiro<sup>2</sup>, Matheus da Silva Campelo<sup>3</sup>, Wesley Lyeverton Correia Ribeiro<sup>4</sup>, Ana Carolina Fonseca Lindoso Melo<sup>5</sup>, Letícia Oliveira da Rocha<sup>6,7</sup>, Maria Elenir Nobre Pinho Ribeiro<sup>3</sup>, Nágila Maria Pontes Silva Ricardo<sup>3</sup>, Flávia Oliveira Monteiro da Silva Abreu<sup>2</sup>, Lorena Mayana Beserra de Oliveira<sup>1</sup>, Weibson Paz Pinheiro André<sup>1</sup>  and Claudia Maria Leal Bevilaqua<sup>1</sup> 

<sup>1</sup>Laboratório de Doenças Parasitárias, Programa de Pós-Graduação em Ciências Veterinárias, Universidade Estadual do Ceará, Fortaleza, Brazil; <sup>2</sup>Laboratório de Química Analítica e Ambiental, Programa de Pós-Graduação em Ciências Naturais, Universidade Estadual do Ceará, Fortaleza, Brazil; <sup>3</sup>Laboratório de Polímeros e Inovação de Materiais, Departamento de Química Orgânica e Inorgânica, Universidade Federal do Ceará, Fortaleza, Brazil; <sup>4</sup>Departamento de Fisiologia e Farmacologia, Faculdade de Medicina, Universidade Federal do Ceará, Fortaleza, Brazil; <sup>5</sup>Departamento de Patologia e Medicina Legal, Faculdade de Medicina, Universidade Federal do Ceará, Fortaleza, Brazil; <sup>6</sup>Laboratório de Biologia Celular e Tecidual, Centro de Biotecnologia e Biotecnologia, Universidade Estadual do Norte Fluminense, Rio de Janeiro, Brazil and <sup>7</sup>Laboratório de Ecotoxicologia, Centro de Ciências Exatas, Naturais e da Saúde, Universidade Federal do Espírito Santo, Vitória, Brazil

### Abstract

This work aimed to evaluate the *in vitro* anthelmintic effect of carvone nanoemulsions on *Haemonchus contortus*. Three R-carvone nanoemulsions were prepared: uncoated R-carvone nanoemulsions homogenized in a sonicator (UNAlg-son) and homogenized in an ultrahomogenizer (UNAlg-ultra) and sodium alginate-coated R-carvone (CNAlg-ultra). The physico-chemical characterizations of the nanoemulsions were carried out. The anthelmintic activity was evaluated using egg hatch test (EHT), larval development test (LDT) and adult worm motility test (AWMT). Changes in cuticle induced in adult *H. contortus* were evaluated by scanning electron microscopy (SEM). The results were subjected to analysis of variance and compared using the Tukey test ( $P < 0.05$ ). The effective concentration to inhibit 50% (EC<sub>50</sub>) of egg hatching and larval development was calculated. The particle sizes were 281.1 nm (UNAlg-son), 152.7 nm (UNAlg-ultra) and 557.8 nm (CNAlg-ultra), and the zeta potentials were  $-15$  mV (UNAlg-son),  $-10.8$  mV (UNAlg-ultra) and  $-24.2$  mV (CNAlg-ultra). The encapsulation efficiency was  $99.84 \pm 0.01\%$ . SEM of the nanoemulsions showed an increase in size. In EHT, the EC<sub>50</sub> values of UNAlg-son, UNAlg-ultra and CNAlg-ultra were 0.19, 0.02 and 0.17 mg mL<sup>-1</sup>, respectively. In LDT, they were 0.29, 0.31 and 0.95 mg mL<sup>-1</sup> for UNAlg-son, UNAlg-ultra and CNAlg-ultra, respectively. The adult motility inhibition was 100% after 12 h of exposure to UNAlg-ultra and CNAlg-ultra, while for UNAlg-son, it was 79.16%. SEM showed changes in the buccal capsule and cuticular damage. It was concluded that R-carvone nanoemulsions showed antiparasitic action demonstrating promise for the control of infections caused by gastrointestinal nematodes in small ruminants.

### Introduction

Gastrointestinal nematode infections (GNIs) are one of the main causes of economic losses for sheep and goats worldwide. Among nematodes, *Haemonchus contortus* is considered the most pathogenic, as it is a haematophagous parasite that causes anaemia, submandibular oedema and, in more severe cases, can lead to death (Wang *et al.*, 2017; Toscano *et al.*, 2018). The control of *H. contortus* is mainly based on the use of synthetic anthelmintics. However, the intensive use of these drugs and inadequate management have resulted in the selection of resistant and multiresistant nematode populations worldwide (Jackson and Coop, 2000; Bartram *et al.*, 2012; Kaplan and Vidyashankar, 2012; Kotze and Prichard, 2016; Tuersong *et al.*, 2020). Thus, new control strategies are being implemented, such as the use of essential oils from plants and their bioactive compounds (Ribeiro *et al.*, 2015; Ferreira *et al.*, 2016; Araújo-Filho *et al.*, 2019).

Essential oils are complex mixtures of active substances of plant origin that exhibit a variety of properties, such as anthelmintic effects, due to the synergism of their compounds (Zhu *et al.*, 2013; Katiki *et al.*, 2017). Studies evaluating the anthelmintic efficacy of compounds isolated from essential oils, such as monoterpenes e.g. carvacrol, thymol, terpinen-4-ol, limonene and carvone, have demonstrated *in vitro* and *in vivo* effects on *H. contortus* (André *et al.*, 2016; Grando *et al.*, 2016; Katiki *et al.*, 2017, 2019; André *et al.*, 2018; Garbin *et al.*, 2021; Silva

*et al.*, 2021). Carvone is a monoterpene that can be found as the main active component of several essential oils, *Mentha spicata* L., *Anethum graveolens* L., *Carum carvi* L. and *Lippia alba* (De Sousa *et al.*, 2007; Johri, 2011). However, one of the limiting factors for the use of this biocompound is its volatility, instability and low water solubility. Thus, an alternative to improve these characteristics is encapsulation in biopolymer matrices (Lertsutthiwong and Rojsithisak, 2011).

Nanoemulsions containing bioactive compounds form nanostructured systems that improve physicochemical stability, modulation of release rates and bioavailability of active principles (Abreu *et al.*, 2020). For nanoencapsulation, biopolymers such as sodium alginate are used. It is a natural polysaccharide extracted from brown marine algae, red algae or bacteria. It has been used as an encapsulating matrix because it is a biodegradable polymer that is biocompatible, is sensitivity to pH, has low toxicity and promotes the controlled release of drugs (Wong *et al.*, 2000; Prabaharan, 2015; Martins *et al.*, 2017; Cheng *et al.*, 2020; Hariyadi and Islam, 2020). The composition of formulations, method and preparation conditions are intrinsically related (Lovelyn and Attama, 2011). Thus, the comparison between the preparation methods of nanoemulsions is advantageous, as it allows obtaining more stable nanoemulsions and efficient controlled release systems (Abreu *et al.*, 2020).

Therefore, the objective of this work was to evaluate the anthelmintic activity of R-carvone nanoemulsions produced by different homogenization methods towards *H. contortus* *in vitro*.

## Materials and methods

### Preparation of nanoemulsions

R(-)-Carvone nanoemulsions (Quinari®, Ponta Grossa, Paraná, Brazil) were prepared by the high-energy emulsification method with 2 different homogenization techniques (high-pressure homogenization and ultrasound) using the following equipment: an ultrahomogenizer ULTRA380 (Ultrastirrer, Jacareí, São Paulo, Brazil) and a sonicator Fisherbrand™ Model 50 Sonic Dismembrator (Thermo Fisher Scientific, Waltham, Massachusetts, EUA) with or without the addition of sodium alginate (Dinâmica, Indaiatuba, São Paulo, Brazil) as a polymer matrix. For the preparation of the uncoated R-carvone nanoemulsion with sodium alginate (UNAlg-son), R-carvone and Tween 80 (Dinâmica, Indaiatuba, São Paulo, Bra) were added at a proportion of 1:15. Then, they were homogenized in a sonicator (Fisherbrand™ Model 50 Sonic Dismembrator) for 5 min at an amplitude of 30  $\mu\text{m}$ . For preparation of the uncoated R-carvone nanoemulsion with sodium alginate (UNAlg-ultra), Tween 80 and R-carvone were added at a proportion of 1:2. Then, they were placed in an ultrasonic eco-sonics Q1.8/25 (Indaiatuba, São Paulo, Brazil) bath for 5 min and homogenized in an ultrahomogenizer ULTRA380 (Ultrastirrer) at 18 000 rpm for 2 min. To prepare the sodium alginate-coated R-carvone nanoemulsion (CNAlg-ultra), 4% sodium alginate, Tween 80 and R-carvone were added in proportions of 1:1:4. The solution was subjected to an ultrasonic bath (Q1.8/25, Ultronique) for 5 min and then homogenized in an ultrahomogenizer (ULTRA380, Ultrastirrer) at 22 000 rpm for 5 min.

### Stability of nanoparticles

The physical stability of the emulsions homogenized in an ultrahomogenizer (UNAlg-ultra and CNAlg-ultra) was evaluated at 1, 7, 14, 21, 30, 60 and 90 days after preparation. For this procedure, ~10 mL of each of the nanoemulsions was maintained in closed test tubes, without exposure to light, at a temperature of 26°C. Periodic observation was implemented to detect any visual signs

of instability, such as creaming, sedimentation or phase separation. Creaming and sedimentation were measured over time with the aid of a caliper. The creaming index (CI) and sedimentation index (SI) were determined by relating the height in centimetres of the precipitates formed in the test tube ( $H_a$ ) with the total height of the sample ( $H_t$ ) after the mentioned preparation periods, calculated according to equations (1) and (2), adapted from Mwangi *et al.* (2016):

$$\text{CI (\%)} = H_a/H_t \times 100 \quad (1)$$

$$\text{SI (\%)} = H_a/H_t \times 100 \quad (2)$$

### Encapsulation efficiency

The encapsulation efficiency (EE) was determined by the difference between the initial amount of carvone in the nanoemulsion and the quantified free amount after ultracentrifugation (8000 rpm for 30 min) (equation (3)) using an Amicon® filter (molecular weight cutoff of 100 kDa, Millipore, UK) (Campelo *et al.*, 2021). In the assay, an aliquot of 1 mL of each nanoemulsion (equivalent to 1.65 mg of carvone) was centrifuged, and the absorbance was determined at 235 nm ( $\lambda_{\text{max}}$  of carvone) using a Genesys 6 Spectrophotometers (Thermo Fisher Scientific, Waltham, Massachusetts, EUA). The %EE was determined from a previously prepared carvone standard curve at concentrations ranging from 2 to 18  $\mu\text{g mL}^{-1}$  ( $y = 0.0678 - 0.016x$ ;  $R^2 = 0.9995$ ). The maximum wavelength obtained in the spectrophotometric scan of carvone was  $\lambda = 235$  nm. From the constructed standard curve, it was possible to determine the content of encapsulated carvone in the nanoemulsion as well as the EE. The experiment was carried out in triplicate, and the results are expressed as the mean  $\pm$  standard error:

$$\text{EE (\%)} = [(\text{Total amount of drug} - \text{free drug}) / \text{Total amount of drug}] \times 100 \quad (3)$$

### Physicochemical characterization of nanoemulsions

Particle size and zeta potential were determined by dynamic light scattering using the Malvern Zetasizer/Nanoseries Z590 equipment.

Detection of the main vibrational stretching modes was carried out by means of spectroscopy in the infrared region by Fourier transform (FTIR). Sample readings were performed on a Shimadzu spectrometer from 400 to 4000  $\text{cm}^{-1}$  using KBr inserts.

Scanning electron microscopy (SEM) of nanoemulsions was performed after 42 days of production. A Zeiss 940A microscope was used at an accelerating voltage of 20 kV and a magnification of 100–3000 $\times$ . Approximately 200  $\mu\text{L}$  of nanoemulsions were placed on rounded metallic structures and dehydrated in a drying oven at 50°C for ~1 h until a thin sample film was obtained on the coin.

### Haemonchus contortus isolate

The Kokstad (KOK) isolate of *H. contortus* multiresistant to commercial synthetic anthelmintics, benzimidazoles, levamisole and macrocyclic lactones was used (Neveu *et al.*, 2007, 2010; Fauvin *et al.*, 2010; Barrere *et al.*, 2014). The isolate was supplied by the Institut National de Recherche pour l'Agriculture, l'Alimentation, et l'Environnement.

**Table 1.** Particle size, zeta potential and polydispersity index of R-carvone nanoemulsions without polymer matrix (NCS-SM and NCT-SM) and R-carvone with polymer matrix (NCT-CM)

| Nanoemulsion | Particle size (nm) | Zeta potential (mV) | Polydispersity index |
|--------------|--------------------|---------------------|----------------------|
| NCS-SM       | 281.1 ± 78.63      | -15 ± 4.25          | 0.909 ± 0.100        |
| NCT-SM       | 152.7 ± 13.86      | -10.8 ± 21.43       | 0.605 ± 0.047        |
| NCT-CM       | 557.8 ± 21.43      | -24.2 ± 4.65        | 0.576 ± 0.047        |

### Egg hatch test

The egg hatch test (EHT) was performed according to the technique described by Coles *et al.* (2006). For egg recovery, feces were collected directly from the rectal ampoule of a sheep experimentally infected with the KOK isolate and processed according to Hubert and Kerboeuf (1992). Suspensions (250  $\mu$ L) containing ~100 fresh eggs were incubated with the same volume of solutions from the following treatments: G1: UNAlg-son and G2: CNAAlg-ultra, at concentrations ranging from 0.06 to 2.0 mg mL<sup>-1</sup>; G3: UNAlg-ultra, at concentrations ranging from 0.125 to 0.007 mg mL<sup>-1</sup>; G4: 0.025 mg mL<sup>-1</sup> of thiabendazole (Sigma-Aldrich®) (positive control); G5: 3% Tween 80 (negative control) and G6: 4% sodium alginate polymer matrix (negative control). The suspension was incubated for 48 h at 25°C, and 5% Lugol's iodine solution was added to stop the hatching of the larvae. For each treatment and control, 5 replicates and 3 repetitions were performed.

### Larval development test (LDT)

Eggs of *H. contortus* were incubated for 24 h to obtain L1. Solutions consisting of 500  $\mu$ L of L1 (~250 larvae) and equal volumes of the following treatments: G1: UNAlg-son; G2: UNAlg-ultra and G3: CNAAlg-ultra, in concentrations ranging from 0.06 to 2.0 mg mL<sup>-1</sup>; G4: 0.008 mg mL<sup>-1</sup> of ivermectin (Sigma-Aldrich®) (positive control); G5: 3% Tween 80 (negative control) and G6: 4% sodium alginate polymer matrix (negative control), were incubated with GNI-free sheep feces for 6 days at room temperature (27°C) (Camurça-Vasconcelos *et al.*, 2007). After the incubation period, L3 were recovered following the technique described by Roberts and O'Sullivan (1950) and counted

using a microscope. For each treatment and control, 3 repetitions were performed with 5 replicates for each.

### Adult worm motility test

The adult worm motility test (AWMT) was performed according to the method described by Hounzangbe-Adote *et al.* (2005). Adult females of *H. contortus* were collected from the abomasum of a sheep with monospecific infection. Soon after the animal was euthanized, the abomasum was removed, and the parasites were washed with saline solution. The mobile females were transferred to a 24-well plate at a density of 3 specimens per well, to which 1 mL phosphate-buffered saline (PBS) with 4% penicillin/streptomycin (Sigma-Aldrich®) was added and maintained at 37°C in a greenhouse with 5% carbon dioxide. After 1 h, 1 mL of treatment was added to the wells: G1: UNAlg-son; G2: UNAlg-ultra and G3: CNAAlg-ultra, at concentrations ranging from 800 to 100  $\mu$ g mL<sup>-1</sup>; G4: 100  $\mu$ g mL<sup>-1</sup> ivermectin (Sigma-Aldrich®); G5: 3% Tween 80 + PBS (negative control) and G6: 4% sodium alginate polymer matrix (negative control). The plates were maintained in the oven, and after 3, 6 and 12 h of incubation, motility was evaluated using a stereomicroscope. Eight replicates were made for each treatment and control groups.

### SEM of adult *H. contortus*

Nematodes obtained from the AWMT were collected and subjected to SEM. Adult specimens of *H. contortus* were fixed in a 2.5% glutaraldehyde solution in 0.1 M sodium cacodylate buffer for a period of 72 h. After 3 washes in the same buffer, the parasites were dehydrated in a graded ethanol series (10, 20, 30, 60, 70, 80, 90 and 100%, 5 min each). The samples were dried in an EMSCOPE CPD 750, mounted in metal stubs and coated with gold-palladium for 5 min at 100  $\text{\AA}$  min<sup>-1</sup>. Possible changes in the cuticle of the treated parasites were observed with an S450 scanning electron microscope (Hitachi) at an accelerating voltage of 15 kV.

### Statistical analysis

In EHT, inhibition of egg hatching was determined according to the following formula: (number of eggs/number of eggs + number of hatched larvae)  $\times$  100. In LDT, the effect was determined

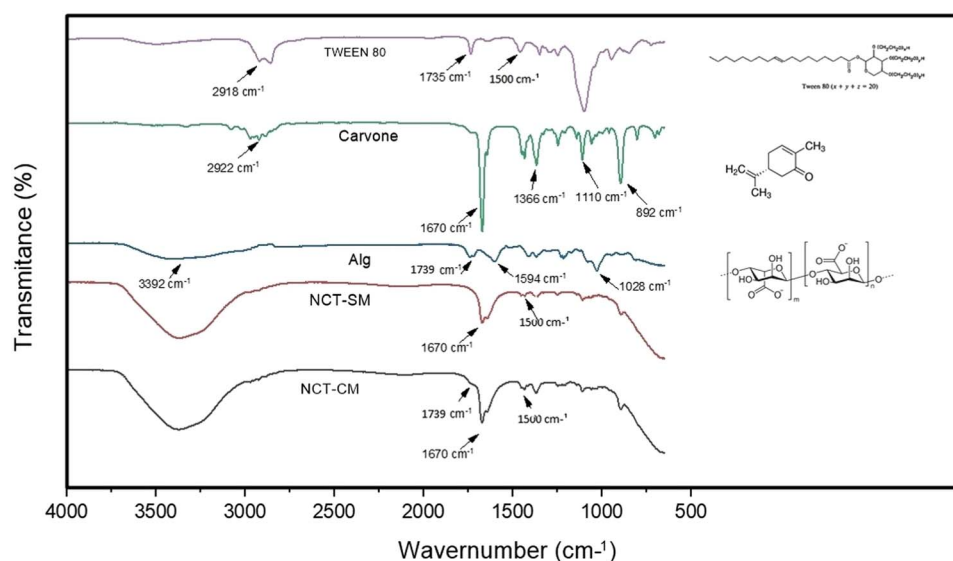


**Fig. 1.** FTIR spectra of carvone, sodium alginate, Tween 80 and uncoated (UNAlg-ultra) and sodium alginate-coated (CNAAlg-ultra) R-carvone nanoemulsions homogenized in an ultrahomogenizer.

according to the following formula: (number of L3 in the negative control – number of L3 in the treated group/number of L3 in the negative control)  $\times 100$ . The percentage of motile adults in AWMT was evaluated as the number of motile worms/total number of worms per well.

In EHT and LDT, the inhibition effects at each concentration of treatment were analysed using analysis of variance (ANOVA) and compared with the Tukey test. To analyse the differences between treatments, the data were subjected to the unpaired *t* test (2-tailed). In AWMT, the inhibition effects at each concentration of treatments at different times were analysed by 2-way ANOVA and compared with the Tukey test, using the SPSS 22.0 program, considering a significance level of 5% ( $P < 0.05$ ).

GraphPad Prism® 6.0 software was used considering a significance level of 5% ( $P < 0.05$ ). Effective concentrations to inhibit 50% ( $EC_{50}$ ) of egg hatching and larval development were calculated by linear regression using the SPSS 22.0 program.

## Results

The macroscopic effects of nanoemulsion stability, such as creaming, sedimentation and phase separation were evaluated, and there was no macroscopic presence of sedimentation phenomena for UNAlg-ultra. For CNAAlg-ultra, it was only possible to observe instability phenomena after 60 days, with a sedimentation rate of 6.6%. Creaming formation was observed only for CNAAlg-ultra 7 days after storage. The CI values were 18.2%

after 7, 14 and 21 days. After 30, 60 and 90 days, the creaming rates varied between 16.1 and 21.5%. In both nanoemulsions, no phase separation phenomenon was observed. The formulations presented nanometric and multimodal particle sizes. The particle size and zeta potential results are shown in Table 1. Samples UNAlg-ultra and UNAlg-son presented an average particle size value of 152.7 and 281.1 nm, respectively; CNAAlg-ultra coated with alginate showed the highest particle size value (557.8 nm).

There was an average content of  $20.24 \pm 1.98\%$  and an average EE of  $99.84 \pm 0.01\%$ . The FTIR spectra of the compounds carvone, Tween 80 and alginate, as well as UNAlg-ultra and CNAAlg-ultra are shown in Fig. 1. Carvone presents the main peaks at  $2922\text{ cm}^{-1}$ , which correspond to the stretching of the methyl groups ( $-\text{CH}_2$ ), as well as at  $1670\text{ cm}^{-1}$ , corresponding to the stretching of the  $\text{C}=\text{C}$  bond, and at  $1445\text{ cm}^{-1}$ , due to the  $\text{C}-\text{H}$  strain. Sodium alginate showed bands at  $3392\text{ cm}^{-1}$  due to the stretching of the  $-\text{OH}$  bond, at  $1739\text{ cm}^{-1}$  corresponding to the stretching of the  $\text{COO}^-$  bond and at  $1028\text{ cm}^{-1}$  attributed to the  $\text{COH}$  stretch. Tween 80 showed the stretching of  $\text{CH}_3$  and  $\text{CH}_2$  groups at  $2918$  and  $2860\text{ cm}^{-1}$ , respectively. Furthermore, it presented an absorption band at  $1735\text{ cm}^{-1}$  due to stretching of the  $\text{C}=\text{O}$  bond, at  $1500\text{ cm}^{-1}$  referring to the angular deformation of the  $-\text{CH}_2$  methyl groups and at  $1095\text{ cm}^{-1}$  due to stretching of the  $\text{COC}$  bond. The aqueous nanoemulsions UNAlg-ultra and CNAAlg-ultra exhibited a combination of peaks from the constituent materials. The peaks at 1670 and

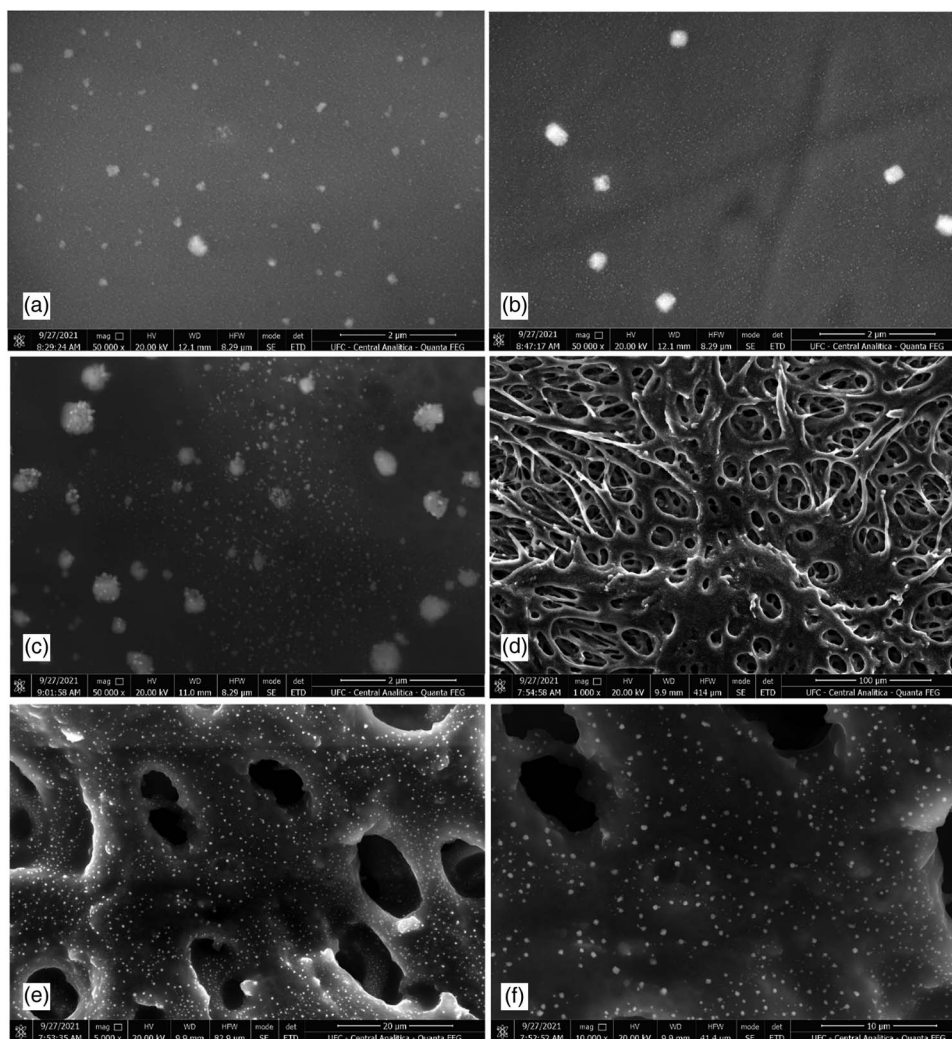


**Fig. 2.** SEM surface images: (a) UNAlg-ultra at 50 000 $\times$ ; (b) UNAlg-son at 50 000 $\times$ ; (c) CNAAlg-ultra at 50 000 $\times$ . Images (d), (e) and (f) show CNAAlg-ultra at different magnifications: 1000 $\times$ , 5000 $\times$  and 10 000 $\times$ .

1336  $\text{cm}^{-1}$  were attributed to C=C and  $-\text{CH}_2$  stretches of carvone, respectively. The peaks at 1500  $\text{cm}^{-1}$  present in Tween were distinctly found in nanoemulsions. The nanoemulsion with sodium alginate matrix CNAIlg-ultra presented a distinction in relation to the nanoemulsion without matrix (UNAIlg-ultra) by the discrete presence of a shoulder at 1739  $\text{cm}^{-1}$ , which could be attributed to stretching of the  $\text{COO}^-$  bond of alginate.

The SEM images of the nanoemulsions are shown in Fig. 2. Figure 2A–C shows the 3 types of nanoemulsions at the same magnification (50 000 $\times$ ). Samples UNAIlg-Ultra and UNAIlg-son showed similar patterns in comparison with the particle size from DLS (Dynamic Light Scattering) results (Table 1). Figure 2A (UNAIlg-ultra) shows micelles with spherical morphology and homogeneously arranged in the medium in which they were dispersed. Figure 2B (UNAIlg-son) shows particles with similar morphology, but with higher particle size, with uneven spacing between micelles. Figure 2C (CNAIlg-ultra) shows the presence of particles with different sizes arranged in a non-uniform manner dispersed along the alginate matrix. Figure 2D–F shows in detail the presence of microspherical inclusions as small particles aggregated to the polymeric matrix network for the sample CNAIlg-ultra, in addition to the formation of structures with porous characteristics in the polymeric network. Figure 2C (UNAIlg-ultra) shows the presence of particles with different sizes arranged in a non-uniform manner in the dispersion medium.

The mean effects of the UNAIlg-son, UNAIlg-ultra and CNAIlg-ultra formulations obtained in the EHT on the *H. contortus*-resistant isolate to synthetic anthelmintics are shown in Fig. 3. At a concentration of 2  $\text{mg mL}^{-1}$ , UNAIlg-son, UNAIlg-ultra and CNAIlg-ultra were 100% effective, showing statistical similarity to the positive control ( $P > 0.05$ ) and a dose-

dependent effect. The  $\text{EC}_{50}$  values of UNAIlg-son, UNAIlg-ultra and CNAIlg-ultra were 0.19, 0.02 and 0.17  $\text{mg mL}^{-1}$ , respectively.

The inhibitory effects of nanoemulsions on LDT are shown in Fig. 4. UNAIlg-son and UNAIlg-ultra inhibited larval development by 100% at a concentration of 2  $\text{mg mL}^{-1}$ , while for CNAIlg-ultra, the inhibition was 80.23%. These results did not differ statistically from the positive control ( $P > 0.05$ ) and showed a dose-dependent effect. The  $\text{EC}_{50}$  values in the LDT for UNAIlg-son, UNAIlg-ultra and CNAIlg-ultra were 0.29, 0.31 and 0.95  $\text{mg mL}^{-1}$ , respectively.

The effects of R-carvone nanoemulsions on the inhibition of *H. contortus* motility are shown in Fig. 5. UNAIlg-ultra and CNAIlg-ultra inhibited worm motility by 100% at a concentration of 800  $\mu\text{g mL}^{-1}$  after 3 h of exposure, while the effectiveness of UNAIlg-son was 79.16% after 12 h of exposure. These results did not differ statistically from the positive control ( $P > 0.05$ ). The motility in the negative (Tween 80 + PBS) and positive controls was 100 and 0%, respectively, at 12 h post-exposure.

SE micrographs (Fig. 6) showed changes in the buccal capsule and along the cuticle of female *H. contortus* after exposure to 800  $\mu\text{g mL}^{-1}$  nanoemulsions. The alterations consisted of the wrinkling of the longitudinal cuticular ridges (Fig. 3B, E and H). There was wrinkling of the buccal capsule and deformation of the lancet (Fig. 3A and G), similar to the positive control (Fig. 3J). The longitudinal cuticular ridges, buccal capsule and lancet seemed to be well preserved in the negative control group (Fig. 3C, F, I and L).

## Discussion

Instability phenomena can limit the period of effective application of emulsified formulations; thus, nanoemulsions based on essential oils require the evaluation of their stability during storage

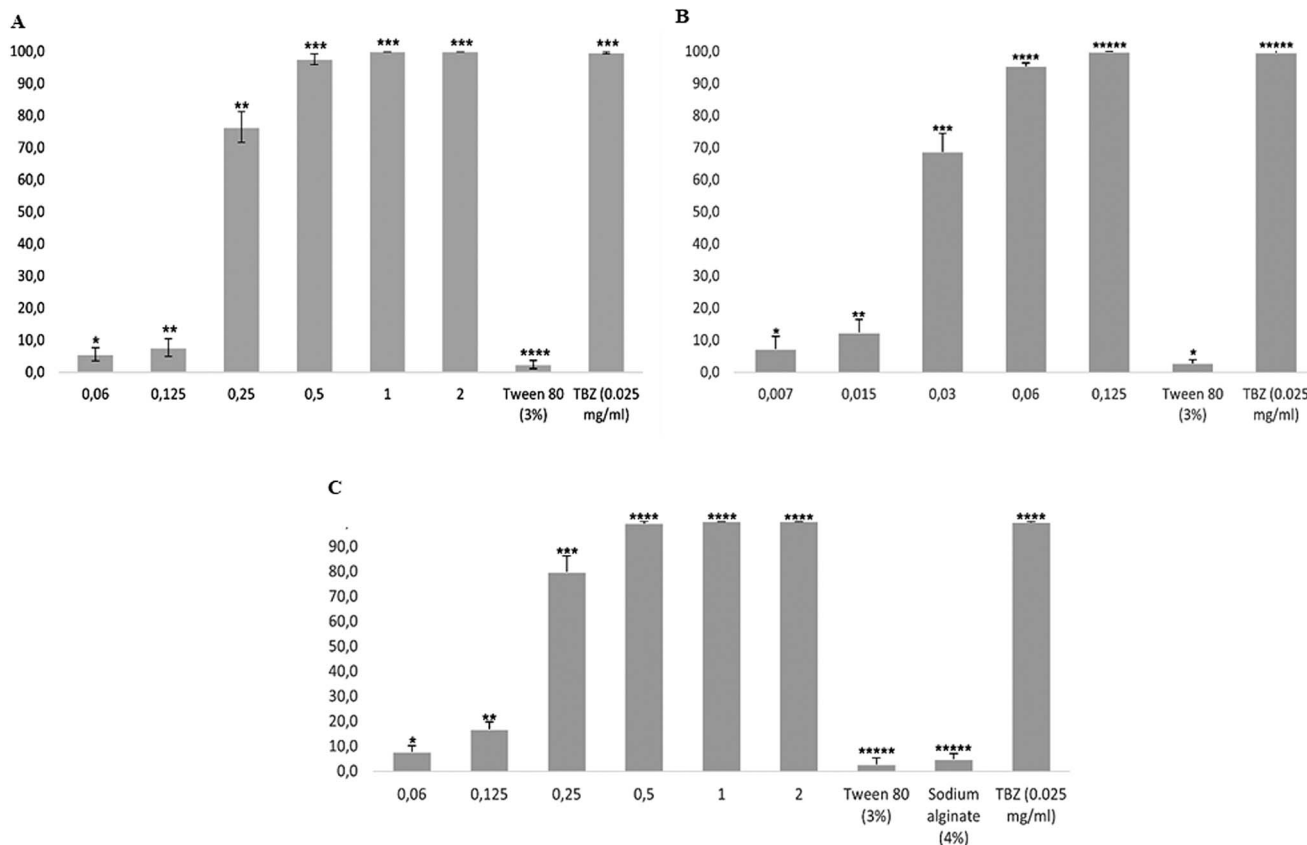


**Fig. 3.** Effects of UNAIlg-son (A), UNAIlg-ultra (B) and CNAIlg-ultra on the hatching of *Haemonchus contortus* eggs. \* Different numbers indicate statistical difference ( $P < 0.05$ ). UNAIlg-son, uncoated R-carvone nanoemulsion with sodium alginate; UNAIlg-ultra, uncoated R-carvone nanoemulsion with sodium alginate; CNAIlg-ultra, sodium alginate coated R-carvone nanoemulsion; TBZ, thiabendazole (positive control). Sodium alginate solution (4%) was used as a negative control for nanoemulsions.

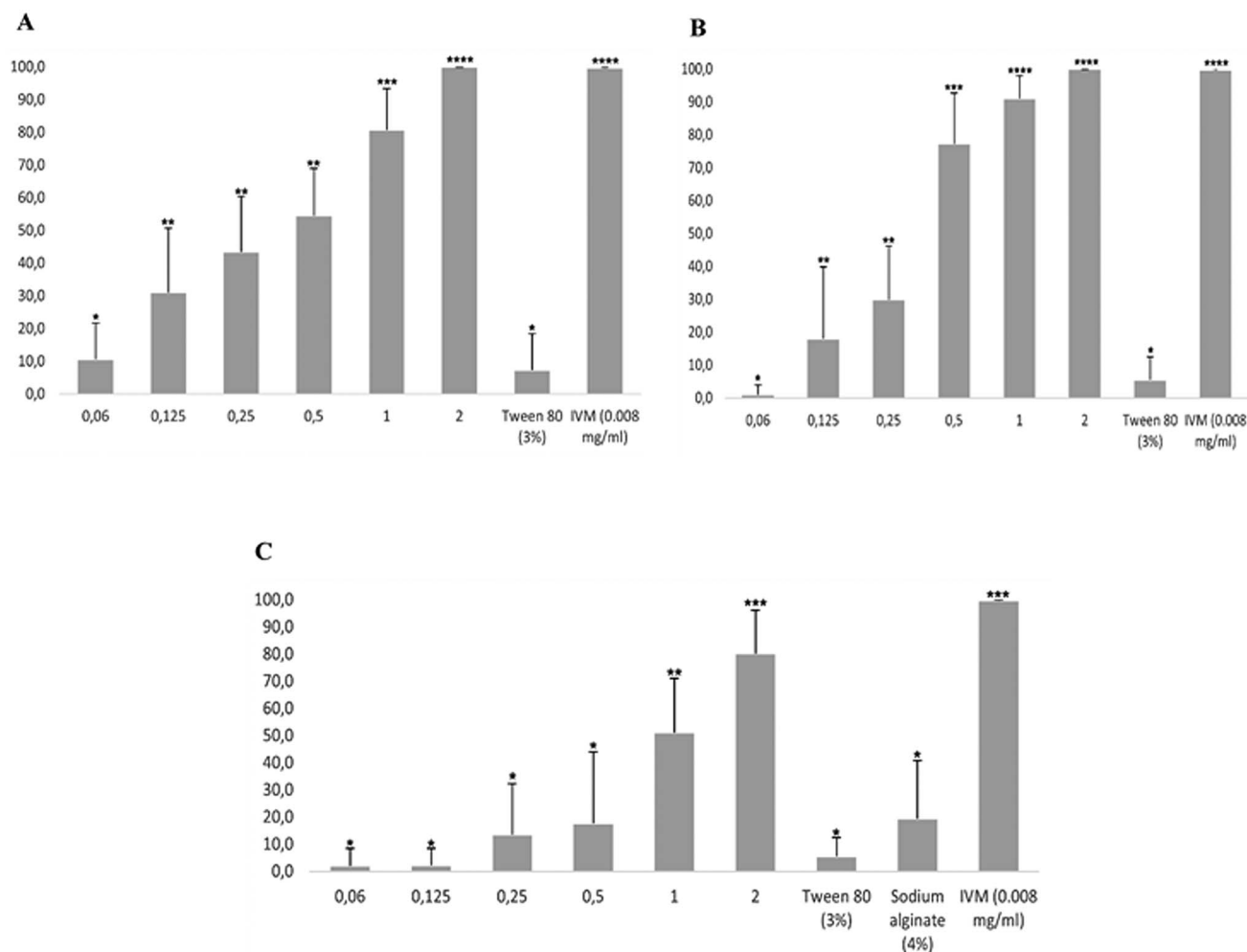


**Fig. 4.** Effects of UNAlg-son (A), UNAlg-ultra (B) and CNAAlg-ultra on larval development of *H. contortus*. \*Different numbers indicate statistical difference ( $P < 0.05$ ). UNAlg-son, uncoated R-carvone nanoemulsion with sodium alginate; UNAlg-ultra, uncoated R-carvone nanoemulsion with sodium alginate; CNAAlg-ultra, sodium alginate coated R-carvone nanoemulsion; IVM, ivermectin (positive control). Sodium alginate solution (4%) was used as a negative control for nanoemulsions.

(Guerra-Rosas *et al.*, 2016). The UNAlg-ultra and CNAAlg-ultra formulations were more stable for sedimentation and creaming phenomena, respectively, as they presented a percentage of secreted volume lower than 1%, even after 90 days of preparation. The formation of creaming in UNAlg-ultra occurred because the nanoemulsion droplets had a lower density than the surrounding liquid, causing an upward movement of the particles, while the sedimentation of CNAAlg-ultra might be due to the larger particle size because of the use of sodium alginate as an encapsulating matrix, in addition to droplets having a higher density than the surrounding liquid, promoting downward movement of the particles (McClements, 2010).

The UNAlg-ultra formulation had the smallest particle size (152.7 nm), followed by UNAlg-son (281.1 nm), while the largest size was found for CNAAlg-ultra (557.8 nm). UNAlg-Ultra and UNAlg-son showed similar pattern sizes in SEM images from lower to higher sizes. In evaluating the morphology of nanoemulsions by SEM, UNAlg-son presented micelles with higher particle size than UNAlg-Ultra ones, which might be due to the instability process causing a possible aggregation of the droplets and, thus, an increase in their size (Daltin, 2011). The formation of porous structures seen in nanoemulsions, and observed in CNAAlg-ultra, is a characteristic of polymeric coating, and has been attributed to the formation of micellar vacuoles in the polymer network (Fernandes *et al.*, 2014; Morais *et al.*, 2016).

The UNAlg-son was homogenized for 5 min, probably because a longer homogenization time could have contributed to

obtaining a smaller particle size (Abismail *et al.*, 1999). To prepare the UNAlg-ultra, the high-pressure homogenization method (ultrahomogenizer) was used, producing a nanoemulsion with a smaller particle size due to the homogenization time (2 min) and rotation speed (18 000 rpm). The particle size decreases as the homogenization time or the rotation speed increases (Benavides *et al.*, 2016). In this case, it is evident that UNAlg-ultra sample showed the lowest particle size, where the ultra-stirrer technique showed higher efficiency in the dispersion of the oily phase in nanometric droplets in comparison with the sonication technique. Although CNAAlg-ultra was prepared with a higher number of revolutions per minute (22 000 rpm) and a longer homogenization time (5 min), this nanoemulsion presented larger particles. Alginate-coated nanoemulsion showed an increased size due to the external polymer matrix which, because of the size of its molecule, promotes the formation of a larger adsorption interface. The alginate matrix involves the nanoemulsion droplets, and despite the occurrence of an increase in the particle size of the nanoemulsion (Salvia-Trujillo *et al.*, 2014), the external coating may prevent from further coalescence stabilizing nanodroplets size for longer periods of time.

Bortoluzzi *et al.* (2020) prepared a nanoemulsion of the essential oil of *Mentha villosa* Hubs (68.8% carvone) using Tween 80 as a surfactant without the addition of a polymer matrix. The sample was first subjected to high-pressure homogenization in an Ultra-Turrax T25 digital IKA (Staufen, Germany) and later in high pressure homogenizer APLAB 10 (Artepeças, São Paulo,

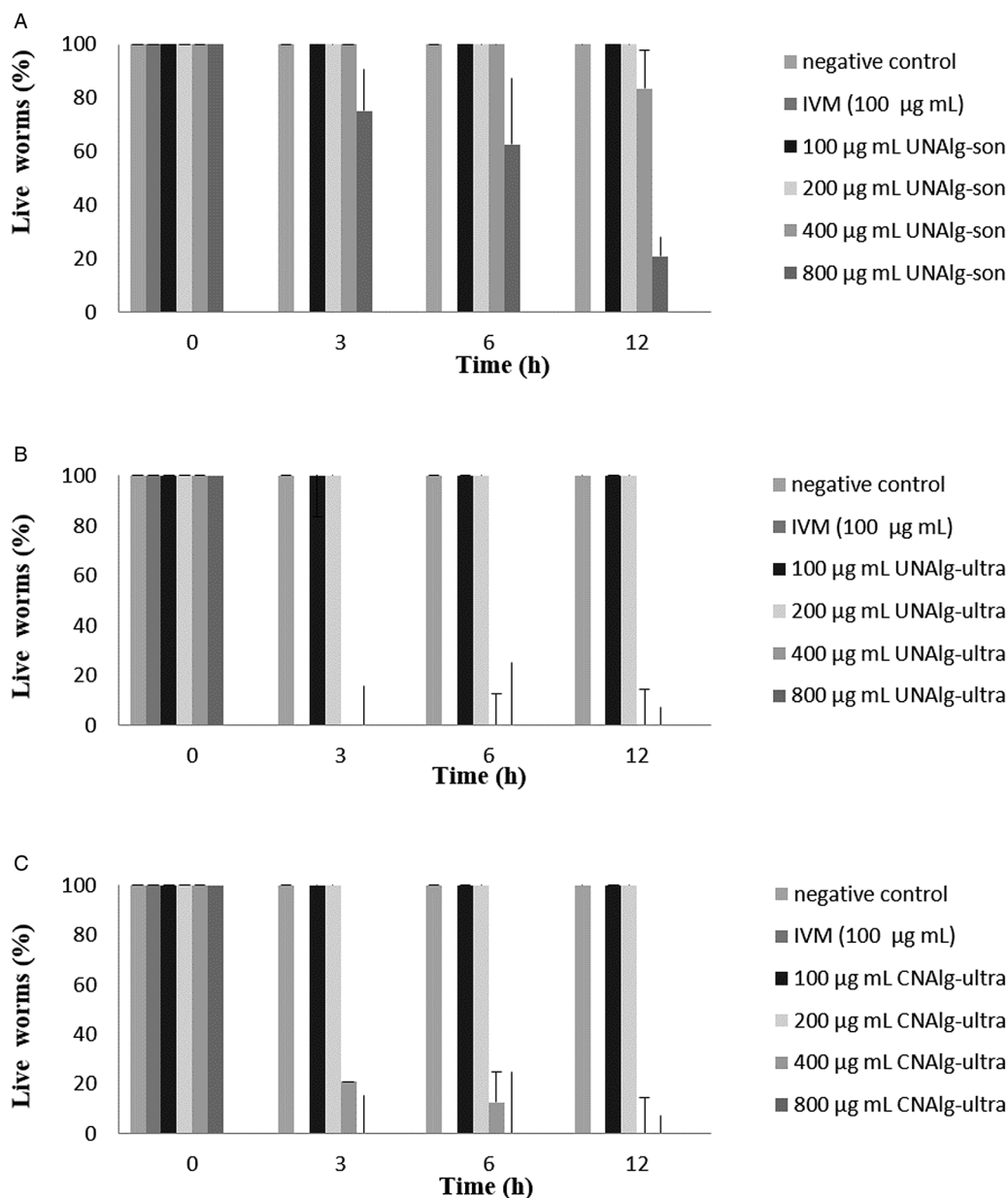


**Fig. 5.** Effects of UNAlg-son (A), UNAlg-ultra (B) and CNAAlg-ultra on adult motility of *H. contortus*. IVM, ivermectin (positive control); Tween 80 + PBS (negative control).

Brazil). This nanoemulsion exhibited a larger particle diameter (164 nm) than the CNAAlg-ultra nanoemulsion utilized in the present study (152.7 nm), prepared without the addition of a polymer matrix. It has been reported that the primary homogenization of the sample and subsequent use of a high-energy homogenization method, such as microfluidization, promotes a significant reduction in particle size (Santos *et al.*, 2018). However, using only 1 high-energy homogenization technique (ultrahomogenizer), it was possible to obtain a slightly smaller particle size compared with the results obtained by Bortoluzzi *et al.* (2020) when using 2 homogenization cycles.

The 3 nanoemulsions had negative zeta potentials, which was related to the use of Tween 80, a nonionic surfactant that can generate a negative charge on oil droplets due to the preferential adsorption of hydroxyl ions from the aqueous phase and sodium alginate, which endows it with a negative charge at neutral pH as an encapsulating matrix (McClements, 2005; Machado *et al.*, 2012; Gago *et al.*, 2019). The zeta potential value of CNAAlg-ultra is close to the recommended stability value, as potentials greater than

+30 mV or less than -30 mV are strongly cationic and anionic, respectively, and are classified as stable (Clogston and Patri, 2011).

The R-carvone nanoemulsion was evaluated for its *in vitro* anthelmintic effect on *H. contortus* eggs, larvae and adults that were multiresistant. The ovicidal effect of UNAlg-ultra was potentiated ( $EC_{50} = 0.02 \text{ mg mL}^{-1}$ ) with homogenization in an ultrahomogenizer without a polymer matrix in comparison with UNAlg-son ( $EC_{50} = 0.18 \text{ mg mL}^{-1}$ ) and CNAAlg-ultra ( $EC_{50} = 0.19 \text{ mg mL}^{-1}$ ). The superior results obtained for the UNAlg-ultra formulation can be explained by its smaller particle size, which possibly allowed greater penetration into the eggshell and, consequently, a better inhibitory effect on larval hatching. The effectiveness of the UNAlg-son and CNAAlg-ultra formulations was similar ( $P > 0.05$ ), indicating that the polymeric system did not enhance the effectiveness of R-carvone on egg hatching. The presence of the sodium alginate matrix as an encapsulating agent in the polymeric system of the UNAlg-ultra may have influenced the controlled release process in the aqueous medium of EHT, prolonging the release of the encapsulated carvone, since the diffusion of drugs retained in the

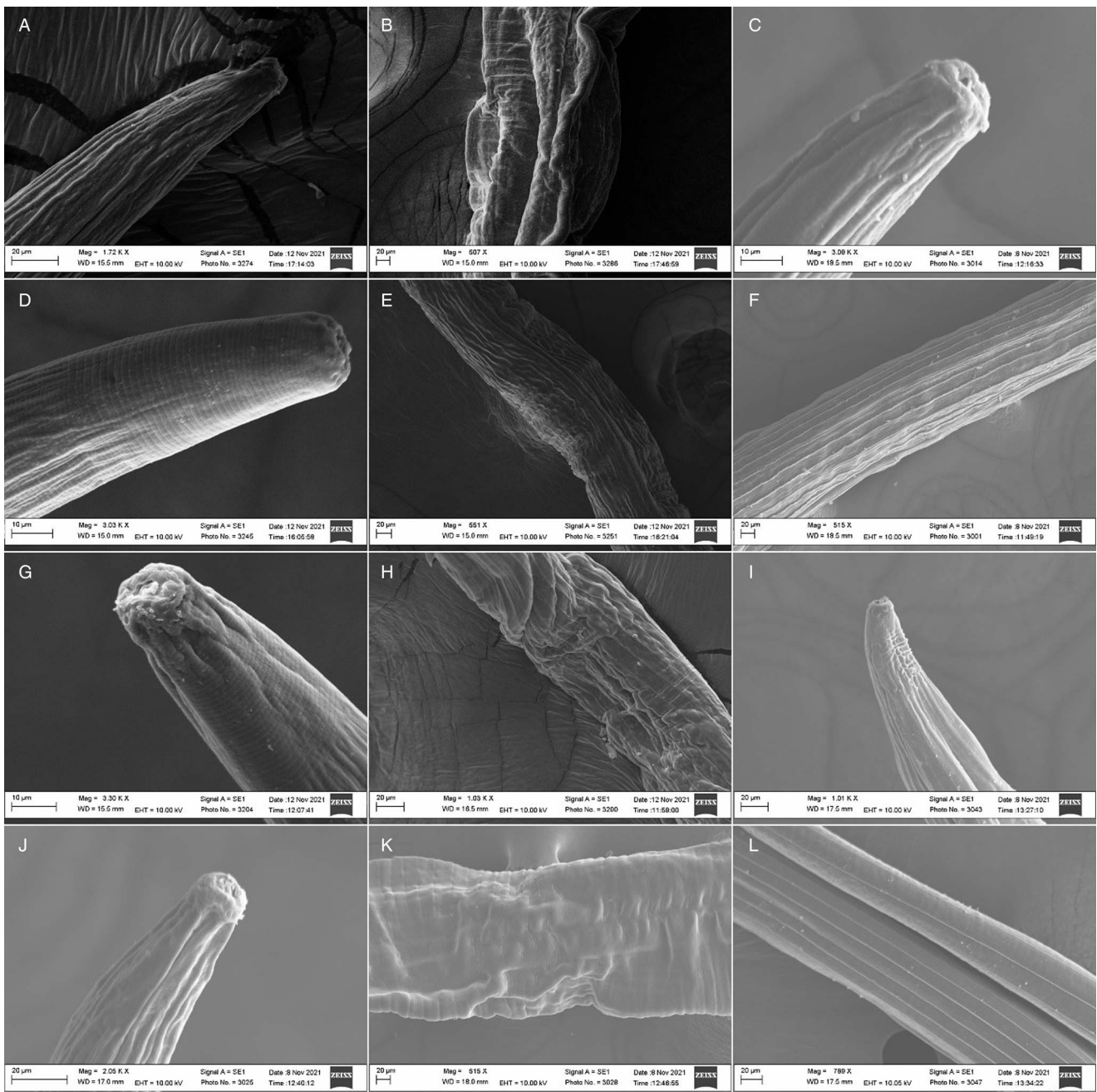


**Fig. 6.** SEM images of ultrastructural changes in the cuticle and cephalic region of adult females of *H. contortus*: (A) and (B) UNAlg-son; (D) and (E) UNAlg-ultra; (G) and (H) CNAAlg-ultra; (C) and (F) Tween 80 + PBS (negative control); (I) and (L) sodium alginate solution 4% (negative control); (J) and (K) ivermectin (positive control).

nanoemulsions occurs when the water enters the polymeric system, resulting in swelling and subsequent release of encapsulated drugs (Dash *et al.*, 2011).

UNAlg-son ( $CE_{50} = 0.29 \text{ mg mL}^{-1}$ ) and UNAlg-ultra ( $CE_{50} = 0.31 \text{ mg mL}^{-1}$ ) formulations showed similar effects ( $P > 0.05$ ), indicating that the type of homogenization did not influence larval development. The CNAAlg-ultra ( $CE_{50} = 0.95 \text{ mg mL}^{-1}$ ) formulation was less effective than the other formulations because the LDT uses a solid medium based on feces, hindering the release of the biocompound from the polymeric system. These results are similar to those of Ribeiro *et al.* (2015), where the nanoemulsion ( $EC_{50} = 2.3 \text{ mg mL}^{-1}$ ) of *Eucalyptus staigeriana* oil had a lower inhibitory effect than the oil in its free form ( $EC_{50} = 1.8 \text{ mg mL}^{-1}$ ).

UNAlg-ultra and CNAAlg-ultra showed a similar effect on the inhibition of adult motility (100%), differing from UNAlg-son,

which only attained 16.65% of the inhibitory effect on adult *H. contortus* motility. This phenomenon may be indicative that high pressurization with an ultrahomogenizer increases the effectiveness of carvone. The use of monoterpenes to inhibit the motility of adult nematodes has been previously reported (André *et al.*, 2016; Araújo-Filho *et al.*, 2018; André *et al.*, 2020). The monoterpenes citronellal and thymol used in the free form completely inhibit the motility of adult *H. contortus* after 12 and 24 h of exposure, respectively (André *et al.*, 2017; Araújo-Filho *et al.*, 2019). We can conclude that the R-carvone nanoemulsion had a better inhibitory effect on adults, since the inhibition was 100% after 3 h of exposure. Thus, the use of encapsulation can potentiate the anthelmintic effect of bioactive compounds and ensure protection for encapsulated substances, making it a useful alternative for controlling multiresistant populations of gastrointestinal nematodes (Ribeiro *et al.*, 2013; Ribeiro *et al.*, 2014).



SEM allowed the observation of damage in the mouth capsule and cuticle of females of *H. contortus* exposed to R-carvone nanoemulsions. Cuticle wrinkling in *H. contortus* caused by exposure to substances with potential anthelmintic effects, such as essential oils, extracts and isolated compounds such as monoterpenes, has been previously described (André *et al.*, 2016, 2017; Ribeiro *et al.*, 2017; Cavalcante *et al.*, 2020). The changes observed in SEM may be related to interactions with the internal structures of nematodes causing physiological disturbances (Brunet *et al.*, 2011), associated with the loss of protective properties of the cuticle, involvement in motility and metabolic changes that occur in the digestive tract of small ruminants (Martínez-Ortiz-de-Montellano *et al.*, 2013).

Some studies suggest that carvone acts as an acetylcholinesterase (AChE) inhibitor (Ryan and Byrne, 1988; Jukic *et al.*, 2007; López and Pascual-Villalobos, 2010; Kurt *et al.*, 2017). Its possible action on AChE receptors observed in vertebrates and invertebrates causes neurotoxic lesions similar to organophosphates, which are potent anthelmintics that are highly toxic to mammals (Miller *et al.*, 1986; Lopez and Pascual-Villalobos, 2010; Ross *et al.*, 2013).

**Acknowledgements.** The authors acknowledge Central Analítica-UFC/CT-INFRA/MCTI-SISANO/Pró-Equipamentos CAPES for the support. Ms Aguiar has received a master research scholarship from Conselho Nacional de Desenvolvimento Científico e Tecnológico (CNPq). Dra Bevilaqua has received a researcher fellowship from CNPq (310663/2016-4-5).

**Author contributions.** A. A. R. M. A., C. M. L. B., W. P. P. A. and L. M. B. O.: conceptualization. A. A. R. M. A., W. P. P. A., J. V. A. F., F. O. M. S. A., H. N. P., W. L. C. R.; A. C. F. L. M., M. E. N. P. R.; N. M. P. S. R.; L. O. R. and L. M. B. O.: performed experiments. A. A. R. M. A., C. M. L. B. and W. P. P. A.: data analysis, supervision and project administration. A. A. R. M. A., C. M. L. B., W. P. P. A. and L. M. B. O.: writing the manuscript. All the authors reviewed and approved the manuscript.

**Financial support.** This study was funded by the Brazilian funding agency Conselho Nacional de Desenvolvimento Científico e Tecnológico (CNPq). Mrs Aguiar received a master's research grant from the National Council for Scientific and Technological Development (130372/2020-0). Dr Bevilaqua is a CNPq fellow (310663/2016-4-5).

**Conflict of interest.** The authors declare that they have no conflicts of interest.

**Ethical standards.** This study was approved by the Ethics Committee for Animal Use of the State University of Ceará (UECE) and registered under protocol number 390620/2020.

## References

- Abismail B, Canselier JP, Wilhelm AM, Delmas H and Gourdon C (1999) Emulsification by ultrasound: drop size distribution and stability. *Ultrasonics Sonochemistry* **6**, 75–83.
- Abreu FOM, Costa EF, Cardial MRL and André WPP (2020) Polymeric nanoemulsions enriched with *Eucalyptus citriodora* essential oil. *Polímeros* **30**, e2020024.
- André WPP, Ribeiro WLC, Cavalcante GS, Santos JML, Macedo ITF, Paula HCB, Freitas RM, Maia SM, Melo JV and Bevilaqua CML (2016) Comparative efficacy and toxic effects of carvacryl acetate and carvacrol on sheep gastrointestinal nematodes and mice. *Veterinary Parasitology* **218**, 52–58.
- André WPP, Cavalcante GS, Ribeiro WLC, Santos JML, Macedo ITF, Paula HCB, Morais SM, Melo JV and Bevilaqua CML (2017) Anthelmintic effect of thymol and thymol acetate on sheep gastrointestinal nematodes and their toxicity in mice. *Revista Brasileira de Parasitologia Veterinária* **26**, 323–330.
- André WPP, Ribeiro WLC, Oliveira LMB, Macedo ITF, Rondon FCM and Bevilaqua CML (2018) Essential oils and their bioactive compounds in the control of gastrointestinal nematodes of small ruminants. *Acta Scientiae Veterinariae* **46**, 552.
- André WPP, Paiva Jr. JR, Cavalcante GS, Ribeiro WLC, Araújo-Filho JV, Cavalcanti BC, Morais SM, Oliveira LMB, Bevilaqua CML and Abreu FOMS (2020) Chitosan nanoparticles loaded with carvacrol and carvacryl acetate for improved anthelmintic activity. *Journal of the Brazilian Chemical Society* **31**, 1614–1622.
- Araújo-Filho JV, Ribeiro WLC, André WPP, Cavalcante GS, Guerra MCM, Muniz CR, Macedo ITF, Rondon FCM, Bevilaqua CML and Oliveira LMB (2018) Effects of *Eucalyptus citriodora* essential oil and its major component, citronellal, on *Haemonchus contortus* isolates susceptible and resistant to synthetic anthelmintics. *Industrial Crops and Products* **124**, 294–299.
- Araújo-Filho JV, Ribeiro WLC, André WPP, Cavalcante GS, Rios TT, Schwinden GM, Rocha IO, Macedo ITF, Morais SM, Bevilaqua CML and Oliveira LMB (2019) Anthelmintic activity of *Eucalyptus citriodora* essential oil and its major component, citronellal, on sheep gastrointestinal nematodes. *Revista Brasileira de Parasitologia Veterinária* **28**, 644–651.
- Barrere V, Beech RN, Charvet CL and Prichard RK (2014) Novel assay for the detection and monitoring of levamisole resistance in *Haemonchus contortus*. *International Journal for Parasitology* **44**, 235–241.
- Bartram DJ, Leathwick DM, Taylor MA, Geurden T and Maeder SJ (2012) The role of combination anthelmintic formulations in the sustainable control of sheep nematodes. *Veterinary Parasitology* **186**, 151–158.
- Benavides S, Cortés P, Parada J and Franco W (2016) Development of alginate microspheres containing thyme essential oil using ionic gelation. *Food Chemistry* **204**, 77–83.
- Bortoluzzi BB, Buzatti A, Chaaban A, Pritsch IC, Anjos AD, Cipriano RR, Deschamps C and Molento MB (2020) *Mentha villosa* Hubs., *M. x piperita* and their bioactives against gastrointestinal nematodes of ruminants and the potential as drug enhancers. *Veterinary Parasitology* **289**, 109317.
- Brunet S, Fourquaux I and Hoste H (2011) Ultrastructural changes in the third-stage, infective larvae of ruminant nematodes treated with sainfoin (*Onobrychis viciifolia*) extract. *Parasitology International* **60**, 419–424.
- Campele MS, Melo EO, Arrais SP, Nascimento FBSA, Gramosa NV, Soares SA, Ribeiro MENP, Silva CR, Júnior HVN and Ricardo NMP (2021) Clove essential oil encapsulated on nanocarrier based on polysaccharide: a strategy for the treatment of vaginal candidiasis. *Colloids and Surfaces A: Physicochemical and Engineering Aspects* **610**, 125732.
- Camurça-Vasconcelos AL, Bevilaqua CM, Morais SM, Maciel MV, Costa CT, Macedo IT, Oliveira LMB, Braga RR, Silva RA and Vieira LS (2007) Anthelmintic activity of *Croton zehntneri* and *Lippia sidoides* essential oils. *Veterinary Parasitology* **148**, 288–294.
- Cavalcante GS, Morais SM, André WPP, Araújo-Filho JV, Muniz CR, Rocha IO, Ribeiro WLC, Rodrigues ALM, Oliveira LMB, Bevilaqua CML and Ramos MV (2020) Chemical constituents of *Calotropis procera* latex and ultrastructural effects on *Haemonchus contortus*. *Revista Brasileira de Parasitologia Veterinária* **29**, 22–25.
- Cheng D, Jiang C, Xu J, Liu Z and Mao X (2020) Characteristics and applications of alginate lyases: a review. *International Journal of Biological Macromolecules* **164**, 1304–1320.
- Clogston JD and Patri AK (2011) Zeta potential measurement. In McNeil S (ed.), *Characterization of Nanoparticles Intended for Drug Delivery. Methods in Molecular Biology (Methods and Protocols)*, **697**, 63–70, Humana Press, New York.
- Coles GC, Jackson F, Pomroy WE, Prichard RK, Von Samsonhimmelstjerna G, Silvestre A, Taylor MA and Vercruyse J (2006) The detection of anthelmintic resistance in nematodes of veterinary importance. *Veterinary Parasitology* **136**, 167–185.
- Daltin D (2011) *Tensoativos: química, propriedades e aplicações*. São Paulo: Edgard Blücher Ltda, 330pp.
- Dash M, Chiellini F, Ottenbrite RM and Chiellini E (2011) Chitosan – a versatile semi-synthetic polymer in biomedical applications. *Progress in Polymer Science* **36**, 981–1014.
- De Sousa DP, Nóbrega FFF and Almeida RN (2007) Influence of the chirality of (R)-(–)- and (S)-(+)-carvone in the central nervous system: a comparative study. *Chirality* **19**, 264–268.
- Fauvin A, Charvet C, Issouf M, Cortet J and Neveu C (2010) cDNA-AFLP analysis in levamisole-resistant *Haemonchus contortus* reveals alternative splicing in a nicotinic acetylcholine receptor subunit. *Molecular and Biochemical Parasitology* **170**, 105–107.
- Fernandes RVDB, Borges SV and Botrel DA (2014) Gum arabic/starch/maltodextrin/inulin as wall materials on the microencapsulation of rosemary essential oil. *Carbohydrate Polymers* **101**, 524–532.

- Ferreira LE, Benincasa BI, Fachin AL, França SC, Contini SS, Chagas AC and Belebony RO (2016) *Thymus vulgaris* L. essential oil and its main component thymol: anthelmintic effects against *Haemonchus contortus* from sheep. *Veterinary Parasitology* **228**, 70–76.
- Gago CML, Artiga-Artigas M, Antunes MDC, Faleiro ML, Miguel MG and Martín-Belloso O (2019) Effectiveness of nanoemulsions of clove and lemongrass essential oils and their major components against *Escherichia coli* and *Botrytis cinerea*. *Journal of Food Science and Technology* **56**, 2721–2736.
- Garbin VP, Munguía B, Saldaña JC, Deschamps C, Cipriano RR and Molento MB (2021) Chemical characterization and *in vitro* anthelmintic activity of *Citrus bergamia* Risso and *Citrus X paradisi* Macfad essential oil against *Haemonchus contortus* Kirby isolate. *Acta Tropica* **217**, 105869.
- Grando TH, De Sá MF, Baldissera MD, Oliveira CB, De Souza ME, Raffin RP, Santos RCV, Domingues R, Minho AP, Leal M and Monteiro SG (2016) *In vitro* activity of essential oils of free and nanostructured *Melaleuca alternifolia* and of terpinen-4-ol on eggs and larvae of *Haemonchus contortus*. *Journal of Helminthology* **90**, 377–382.
- Guerra-Rosas MI, Morales-Castro J, Ochoa-Martinez LA, Salvia-Trujillo L and Olga Martín-Belloso O (2016) Long-term stability of food-grade nanoemulsions from high methoxyl pectin containing essential oils. *Food Hydrocolloids* **52**, 438–446.
- Hariyadi D M and Islam N (2020) Current Status of Alginate in Drug Delivery. *Advances in Pharmacological and Pharmaceutical Sciences* **16**.
- Hounzangbe-Adote MS, Paolini V, Fouraste I, Moutairou K and Hoste H (2005) *In vitro* effects of four tropical plants on three life-cycle stages of the parasitic nematode, *Haemonchus contortus*. *Veterinary Science Research* **78**, 155–160.
- Hubert J and Kerboeuf DA (1992) Microlarval development assay for the detection of anthelmintic resistance in sheep nematodes. *Veterinary Record* **130**, 442–446.
- Jackson F and Coop RL (2000) The development of anthelmintic resistance in sheep nematodes. *Parasitology* **120**, 95–107.
- Johri RK (2011) *Cuminum cyminum* and *Carum carvi*: an update. *Pharmacognosy Review* **5**, 63–72.
- Jukic M, Politeo O, Maksimovic M, Milos M and Milos M (2007) *In vitro* acetylcholinesterase inhibitory properties of thymol, carvacrol and their derivatives thymoquinone and thymohydroquinone. *Phytotherapy Research* **21**, 259–261.
- Kaplan RM and Vidyashankar AN (2012) An inconvenient truth: global warming and anthelmintic resistance. *Veterinary Parasitology* **186**, 70–78.
- Katiki LM, Barbieri AME, Araujo RC, Verissimo CJ, Louvandini H and Ferreira JFS (2017) Synergistic interaction of ten essential oils against *Haemonchus contortus* *in vitro*. *Veterinary Parasitology* **243**, 47–51.
- Katiki LM, Araujo RC, Ziegelmeyer ACP, Gomes G, Gutmanis L, Rodrigues MS, Bueno CJ, Verissimo H, Louvandini JFS and Ferreira AFT (2019) Evaluation of encapsulated anethole and carvone in lambs artificially- and naturally-infected with *Haemonchus contortus*. *Experimental Parasitology* **197**, 36–42.
- Kotze AC and Prichard RK (2016) Anthelmintic resistance in *Haemonchus contortus*: history, mechanisms and diagnosis. *Advances in Parasitology* **93**, 397–428.
- Kurt BZ, Gazioglu L, Dag A, Salmas RE, Kaylk G, Durdagi S and Sonmez F (2017) Synthesis, anticholinesterase activity and molecular modeling study of novel carbamate-substituted thymol/carvacrol derivatives. *Bioorganic & Medicinal Chemistry* **25**, 1352–1363.
- Lertsutthiwong P and Rojsitthisak P (2011) Chitosan-alginate nanocapsules for encapsulation of turmeric oil. *Pharmazie* **66**, 911–915.
- López MD and Pascual-Villalobos MJ (2010) Mode of inhibition of acetylcholinesterase by monoterpenoids and implications for pest control. *Industrial Crops and Products* **31**, 284–288.
- Lovelyn C and Attama AA (2011) Current state of nanoemulsions in drug delivery. *Journal of Biomaterials and Nanobiotechnology* **2**, 626–639.
- Machado AHE, Lundberg D, Ribeiro AJ, Veiga FJ, Lindman B, Miguel MG and Olsson U (2012) Preparation of calcium alginate nanoparticles using water-in-oil (W/O) nanoemulsions. *Langmuir* **28**, 4131–4141.
- Martins E, Poncelet D, Rodrigues RC and Renard D (2017) Oil encapsulation techniques using alginate as encapsulating agent: applications and drawbacks. *Journal of Microencapsulation* **4**, 754–771.
- Martínez-Ortiz-de-Montellano C, Arroyo-López C, Fourquaux I, Torres-Costa CA and Hoste H (2013) Scanning electron microscopy of *Haemonchus contortus* exposed to tannin rich plants under *in vivo* and *in vitro* conditions. *Experimental Parasitology* **133**, 281–286.
- McClements DJ (2005) *Food Emulsions: Principles, Practices, and Techniques*, Vol. 2. Boca Raton: CRC Press, 714pp.
- McClements DJ (2010) Emulsion design to improve the delivery of functional lipophilic components. *Annual Review of Food Science and Technology* **1**, 241–269.
- Miller JE, Baker NF and Farver TB (1986) Anthelmintic treatment of pastured dairy cattle in California. *American Journal of Veterinary Research* **47**, 2036–2040.
- Morais ARV, Alencar EN, Xavier Jr. FH, Oliveira CM, Marcelino HR, Barratt G, Fessi H, Egito EST and Elaissari A (2016) Freeze-drying of emulsified systems: a review. *International Journal of Pharmaceutics* **503**, 102–114.
- Mwangi WW, Ho KW, Tey BT and Chan ES (2016) Effects of environmental factors on the physical stability of pickering-emulsions stabilized by chitosan particles. *Food Hydrocolloids* **60**, 543–550.
- Neveu C, Charvet C, Fauvin A, Cortet J, Castagnone-Sereno P and Cabaret J (2007) Identification of levamisole resistance markers in the parasitic nematode *Haemonchus contortus* using a cDNA-AFLP approach. *Parasitology* **134**, 1105–1110.
- Neveu C, Charvet CL, Fauvin A, Cortet J, Beech RN and Cabaret J (2010) Genetic diversity of levamisole receptor subunits in parasitic nematode species and abbreviated transcripts associated with resistance. *Pharmacogenetics and Genomics* **20**, 414–425.
- Prabaharan M (2015) Chitosan-based nanoparticles for tumor-targeted drug delivery. *International Journal of Biological Macromolecules* **72**, 1313–1322.
- Ribeiro WLC, Macedo ITF, Santos JML, Oliveira EF, Camurça-Vasconcelos ALF, Paula HCB and Bevilaqua CML (2013) Activity of chitosan encapsulated *Eucalyptus staigeriana* essential oil on *Haemonchus contortus*. *Experimental Parasitology* **135**, 24–29.
- Ribeiro JC, Ribeiro WLC, Camurça-Vasconcelos ALF, Macedo ITF, Santos JML, Paula HCB, Araújo-Filho JV, Magalhães RD and Bevilaqua CML (2014) Efficacy of free and nanoencapsulated *Eucalyptus citriodora* essential oils on sheep gastrointestinal nematodes and toxicity for mice. *Veterinary Parasitology* **204**, 243–248.
- Ribeiro WLC, Camurça-Vasconcelos ALF, Macedo ITF, Santos JML, Ribeiro JC, Pereira VA, Viana DA, Paula HCB and Bevilaqua CML (2015) *In vitro* effects of *Eucalyptus staigeriana* nanoemulsion on *Haemonchus contortus* and toxicity in rodents. *Veterinary Parasitology* **212**, 444–447.
- Ribeiro WLC, Camurça-Vasconcelos ALF, Santos JML, Macedo ITF, Ribeiro JC, Oliveira EF, Paula HCB and Bevilaqua CML (2017) The use of *Eucalyptus staigeriana* nanoemulsion for control of sheep haemonchosis. *Pesquisa Veterinária Brasileira* **37**, 221–226.
- Roberts FHS and O'Sullivan JP (1950) Methods for egg counts and larval cultures for strongyles infesting the gastrointestinal tract of cattle. *Australian Journal of Agricultural Research* **1**, 99–102.
- Ross SM, McManus IC, Harrison V and Mason O (2013) Neurobehavioral problems following low-level exposure to organophosphate pesticides: a systematic and meta-analytic review. *Critical Reviews in Toxicology* **43**, 21–44.
- Ryan MF and Byrne O (1988) Plant-insect coevolution and inhibition of acetylcholinesterase. *Journal of Chemical Ecology* **14**, 1965–1975.
- Salvia-Trujillo L, Rojas-Grau MA, Soliva-Fortuny R and Martín-Belloso O (2014) Formulation of antimicrobial edible nanoemulsions with pseudo-ternary phase experimental design. *Food and Bioprocess Technology* **7**, 3022–3032.
- Santos J, Ramírez P, Llinares R, Muñoz J and Trujillo-Cayado LA (2018) Enhancing rosemary oil-in-water microfluidized nanoemulsion properties through formulation optimization by response surface methodology. *LWT* **97**, 370.
- Silva CR, Lifschitz AL, Macedo SRD, Campos NRCL, Viana-Filho M, Alcântara ACS, Araújo JG, Alencar LMR and Costa-Junior LM (2021) Combination of synthetic anthelmintics and monoterpenes: assessment of efficacy, and ultrastructural and biophysical properties of *Haemonchus contortus* using atomic force microscopy. *Veterinary Parasitology* **290**, 109345.
- Toscano JHB, Lopes LG, Giraldeiro LA and Da Silva MH (2018) Identification of appropriate reference genes for local immune-related studies in Morada Nova sheep infected with *Haemonchus contortus*. *Molecular Biology Reports* **45**, 1253–1262.
- Tuersong W, He L, Zhu T, Yang X, Zhang Z, Ahmad AA, Di W, Wang C, Zhou C, Liu H, Chen J and Hu M (2020) Development and evaluation of a

- loop-mediated isothermal amplification (LAMP) assay for the detection of the E198A SNP in the isotype-1  $\beta$ -tubulin gene of *Haemonchus contortus* populations in China. *Veterinary Parasitology* **278**, 109040.
- Wang C, Li F, Zhang Z, Yang X, Ahmad AA, Li X, Du A and Hu M** (2017) Recent research progress in China on *Haemonchus contortus*. *Frontiers in Microbiology* **8**, 1509.
- Wong TY, Preston LA and Schiller NL** (2000) Alginate lyase: review of major sources and enzyme characteristics, structure-function analysis, biological roles, and applications. *Annual Review of Microbiology* **54**, 289–340.
- Zhu L, Dai J, Li Yang L and Qiu J** (2013) Anthelmintic activity of *Arisaema franchetianum* and *Arisaema lobatum* essential oils against *Haemonchus contortus*. *Journal of Ethnopharmacology* **148**, 311–316.